Journal of Organometallic Chemistry, 474 (1994) 191–197

X-ray structural analysis of the polyhydride complex salt $[(Ph_3P)_3Ir(\mu\text{-}H)_3Ag(\mu\text{-}H)_3Ir(Ph_3P)_3][O_3SCF_3]$

F. Bachechi

Istituto di Strutturistica Chimica "G. Giacomello", CNR, Area della Ricerca di Roma, CP10, 0000016 Monterotondo St, Rome (Italy)

(Received September 22, 1993)

Abstract

The polyhydride complex $[(Ph_3P)_3Ir(\mu\text{-}H)_3Ag(\mu\text{-}H)_3Ir(Ph_3P)_3]^+$ has been prepared and characterized as the trifluorosulfonate salt. It crystallizes in the triclinic $P\bar{1}$ space group with $z = 1$; $a = 10.100(4)$, $b = 14.940(4)$, $c = 15.309(5)$ Å; $\alpha = 116.53(4)$, $\beta = 94.55(4)$, $\gamma = 108.43(4)°$ and $V = 2643$ Å^3. The structure consists of a cluster with a linear Ir–Ag–Ir array. The hydride ligands were not located but from the arrangement of the heavy atoms their most probable positions bridging the Ir–Ag interactions were obtained by potential energy methods.

Key words: Iridium; Silver; Hydride; Cluster; X-ray structure

1. Introduction

The mononuclear iridium hydride *fac*-$[(Ph_3P)_3IrH_3]$ reacts with silver ions in a 2:1 ratio forming the trinuclear complex $[(Ph_3P)_3Ir(\mu\text{-}H)_3Ag(\mu\text{-}H)_3\text{-}Ir(Ph_3P)_3]^+$, **1**. The *mer* isomer reacts with Ag^+, but with the same Ir:Ag ratio the product of the reaction is not complex **1**. A new compound formed which could not be characterized, but which transformed to **1** over a few hours [1].

In solution, **1** is highly fluxional on the NMR time scale, and single resonances were observed for the six equivalent phosphorus and six equivalent hydride ligands. However, the IR spectra on solid samples suggested the presence of two types of hydride. An absorption band at 2100 cm^{-1} is considered due to terminal hydrides, and two bands at 1970 and 1900 cm^{-1} to bridging hydrides [1]. Similar features were observed in the IR spectra of other trinuclear polyhydrides, $[(Me_2PhP)_3HIr(\mu\text{-}H)_2Ag(\mu\text{-}H)_2IrH(Me_2PhP)_3]^+$ and $[(Me_2PhP)_3HIr(\mu\text{-}H)_2Cu(\mu\text{-}H)_2IrH(Me_2PhP)_3]^+$, **2**, [2] and $[(\text{triphos})HRh(\mu\text{-}H)_2Ag(\mu\text{-}H)_2RhH(\text{triphos})]^+$, **3**, and $[(\text{triphos})HRh(\mu\text{-}H)_2Cu(\mu\text{-}H)_2RhH(\text{triphos})]^+$, **4**, where triphos is the tridentate phosphine $CH_3C\{Ph_2CH_2P\}_3$ [3]. The crystal structure analyses of **2**, **3** and **4** did not allow the localization of the hydrides, but the heavy atoms arrangements, though different in **2** compared to **3** and **4**, were compatible with the presence of both terminal and bridging hy-

TABLE 1. Crystallographic data

Formula	$C_{109}H_{96}O_3F_3P_6SAgIr_2$
Mol. wt.	2221.1
a (Å)	14.100(4)
b (Å)	14.940(4)
c (Å)	15.309(5)
α (°)	116.53(4)
β (°)	94.55(4)
γ (°)	108.43(4)
V (Å^3)	2643
Z	1
Crystal system	Triclinic
Space group	$P\bar{1}$
Density calcd. (g cm^{-3})	1.395
Crystal dimensions (mm^3)	0.45 × 0.30 × 0.60
Radiation graphite-monochromated Mo Kα	$\lambda = 0.71069$ Å
Absorption coefficient (cm^{-1})	28.43
Scan mode	ω-scan
Scan range (°)	1.0
Scan speed	variable according the intensity
Background counts	0.5 scan time at ±0.8°
Intensity control standard	3 of every 100 reflections measured
2θ angle (°)	3–56
Total no. of observations	18540
No. of unique data with $I \geq 3\sigma(I)$	9677
Data/parameters	16
No. parameters refined	595
R	0.069
R_w	0.079

0022-328X/94/$7.00
SSDI 0022-328X(93)24263-5

TABLE 2. Final atomic coordinates with their eds values in parentheses

	x	y	z
AG	0.0000	0.0000	0.0000
IR	0.13479(3)	0.21095(3)	0.10801(3)
P(1)	0.0807(2)	0.3215(2)	0.0608(2)
P(2)	0.2933(2)	0.2234(2)	0.0637(2)
P(3)	0.1705(2)	0.2955(2)	0.2860(2)
C(1)	0.1747(8)	0.4251(9)	0.0429(9)
C(2)	0.167(1)	0.432(1)	−0.043(1)
C(3)	0.243(1)	0.514(2)	−0.051(2)
C(4)	0.323(1)	0.591(1)	0.027(2)
C(5)	0.332(1)	0.589(1)	0.118(1)
C(6)	0.2604(9)	0.507(1)	0.125(1)
C(7)	0.0161(8)	0.399(1)	0.1471(8)
C(8)	0.040(1)	0.510(1)	0.179(1)
C(9)	−0.008(1)	0.567(1)	0.246(1)
C(10)	−0.080(2)	0.514(2)	0.281(1)
C(11)	−0.107(1)	0.406(2)	0.250(1)
C(12)	−0.0530(9)	0.347(1)	0.180(1)
C(13)	−0.0237(7)	0.2448(9)	−0.0582(8)
C(14)	−0.038(1)	0.144(1)	−0.1345(9)
C(15)	−0.116(1)	0.091(1)	−0.224(1)
C(16)	−0.181(1)	0.136(1)	−0.238(1)
C(17)	−0.169(1)	0.239(1)	−0.161(1)
C(18)	−0.091(1)	0.292(1)	−0.072(1)
C(19)	0.3032(8)	0.251(1)	−0.0412(8)
C(20)	0.231(1)	0.176(1)	−0.1348(9)
C(21)	0.234(1)	0.190(2)	−0.216(1)
C(22)	0.314(2)	0.281(2)	−0.208(1)
C(23)	0.324(1)	0.355(2)	−0.118(1)
C(24)	0.381(1)	0.340(1)	−0.035(1)
C(25)	0.4208(7)	0.3211(9)	0.1540(8)
C(26)	0.509(1)	0.298(1)	0.151(1)
C(27)	0.604(1)	0.381(2)	0.219(2)
C(28)	0.527(1)	0.504(1)	0.294(1)
C(29)	0.611(1)	0.481(2)	0.289(1)
C(30)	0.4295(9)	0.423(1)	0.226(1)
C(31)	0.3101(9)	0.093(1)	0.010(1)
C(32)	0.363(1)	0.065(2)	−0.064(2)
C(33)	0.375(2)	−0.038(2)	−0.099(2)
C(34)	0.338(2)	−0.105(2)	−0.058(3)
C(35)	0.289(2)	−0.077(1)	0.010(2)
C(36)	0.272(1)	0.020(1)	0.046(1)
C(37)	0.0534(8)	0.274(1)	0.3328(8)
C(38)	0.043(1)	0.358(1)	0.4177(9)
C(39)	−0.050(1)	0.335(1)	0.448(1)
C(40)	−0.128(1)	0.234(2)	0.398(1)
C(41)	−0.117(1)	0.151(1)	0.317(1)
C(42)	−0.027(1)	0.172(1)	0.284(1)
C(43)	0.2373(9)	0.2366(9)	0.3409(8)
C(44)	0.314(1)	0.206(1)	0.302(1)
C(45)	0.370(1)	0.165(1)	0.343(1)
C(46)	0.348(1)	0.156(1)	0.426(1)
C(47)	0.273(2)	0.187(2)	0.466(1)
C(48)	0.217(1)	0.227(1)	0.425(1)
C(49)	0.2490(8)	0.4423(9)	0.3708(8)
C(50)	0.339(1)	0.482(1)	0.444(1)
C(51)	0.396(1)	0.592(1)	0.503(1)
C(52)	0.367(1)	0.666(1)	0.489(1)
C(53)	0.276(1)	0.626(1)	0.418(1)
C(54)	0.2172(9)	0.517(1)	0.3601(9)
C(55)	0.379(1)	0.9843(9)	0.574(1)
S	0.476(2)	1.104(2)	0.663(2)
F(1)	0.288(2)	0.980(2)	0.546(2)
F(2)	0.378(5)	0.917(5)	0.620(5)
F(3)	0.399(5)	0.970(6)	0.483(5)
O(1)	0.477(4)	1.197(3)	0.646(4)
O(2)	0.473(4)	1.145(4)	0.758(3)
O(3)	0.571(4)	1.101(6)	0.662(5)

drides. The X-ray analysis of **1** was undertaken and features similar to those observed in the other trinuclear polyhydrides were expected, although in this case the IR band in the terminal hydride region was quite weak.

2. Experimental details

2.1. *Synthesis and characterisation of $[(Ph_3P)_3Ir(\mu\text{-}H)_3Ag(\mu\text{-}H)_3Ir(Ph_3P)_3][CF_3SO_3]$*

A solution of 26 mg (0.1 mmol) $AgCF_3SO_3$ in 2 ml THF was added to a solution of 186 mg (0.2 mmol) *fac*-$[(Ph_3P)_3IrH_3]$ in 5 ml CH_2Cl_2 at room temperature. The mixture was stirred and slightly warmed for 5 min and then filtered. Hexane was added until development of slight turbidity. The mixture was kept at −20°C. After 12 h small, colourless crystals appeared, which were filtered off and washed with pentane.

Anal. calcd. for $C_{109}H_{90}AgF_3Ir_2O_3P_6S$ (2215.09): C, 59.10, H 4.10. Found: C, 58.76, H, 4.33%. $^{31}P\{^1H\}$ NMR (CD_2Cl_2, 0°C): 3.35 ppm (d, $^2J(Ag, P) = 24.5$ Hz). ^1H (CD_2Cl_2, 0°C): 6.7–7.9 ppm (m, arom.), −11.3 ppm (m, hydrides). $^1J(^{107}Ag, H) = 52$ Hz, $^1J(^{109}Ag, H) = 59$ Hz). IR: 2100, 1970, 1900 cm^{-1}.

The crystals used for the X-ray analysis were recrystallized by slow evaporation of a solution of the complex in ethanol.

2.2. *Collection and reduction of X-ray intensity data*

The X-ray analysis was undertaken on colourless crystals, which were found to be triclinic, space group $P\bar{1}$. A prismatic crystal of *ca.* 0.45 × 0.30 × 0.60 mm was sealed in a glass capillary with its mother liquor and used for the collection of data. The unit-cell dimensions were determined by a least-squares refinement of the setting angles of 15 high-angle reflections ($20 > 2\theta < 26°$) carefully centred. The intensities were collected on a Nicolet R3 computer-controlled diffractometer using graphite-monochromatized Mo Kα radiation in the ω-scan mode at variable scan rate. Three standards were measured every 100 reflections and were found to remain constant. All the reflections were processed to yield values of I and $\sigma(I)$ [4]; in the estimation of $\sigma(I)$ the uncertainty factor $p = 0.013$ was calculated from the variance of the standard reflections [5]. Corrections for Lorentz and polarization were applied. An empirical absorption correction [6] was applied using scan data of three reflections at χ angles of 88.2°. The minimum normalized transmission factors were in the range 0.66–0.70. Only the independent reflections which met the conditions $I > 3\sigma(I)$ were used in the subsequent calculations. In Table 1 the crystallographic data are summarized.

2.3. Solution and refinement of the structure

The structure was solved by the heavy atom method and refined by full-matrix least-squares procedures with the minimized function $\Sigma w(| F_o | - | F_c |)^2$, where $w = 1/\sigma^2(F_o^2)$. After convergence of the isotropic refinement at $R = 0.098$, the hydrogen atoms were introduced into calculated positions and refined riding on the corresponding carbon atoms. All the non-hydrogen atoms were allowed to vibrate anisotropically. All the hydrogen atoms were given the isotropic thermal factors of the parent carbon atoms, which were not refined. A Fourier difference map at this point revealed a few weak peaks which could be interpreted as due to the disordered half molecule per asymmetric unit of $[CF_3SO_3]^-$. The final cycles of refinements, which include the $[CF_3SO_3]^-$ group with 0.5 occupancy, converged at $R = 0.069$ and $R_w = 0.070$. All calculations were performed on a Data General Eclipse MV8000II computer using local programs. Scattering factors and anomalous dispersion terms were taken from the *International Tables for X-Ray Crystallography* [7]. Final atomic parameters of the non-hydrogen atoms are given in Table 2. Full lists of bond lengths and angles, hydrogen atom coordinates and thermal parameters have been deposited with the Cambridge Crystallographic Data Centre. The authors will also supply these and lists of structure factors.

3. Results and discussion

The crystal structure of $[(PPh_3)_3Ir(\mu\text{-}H)_3Ag(\mu\text{-}H)_3Ir(PPh_3)_3][CF_3SO_3]$, consists of the packing

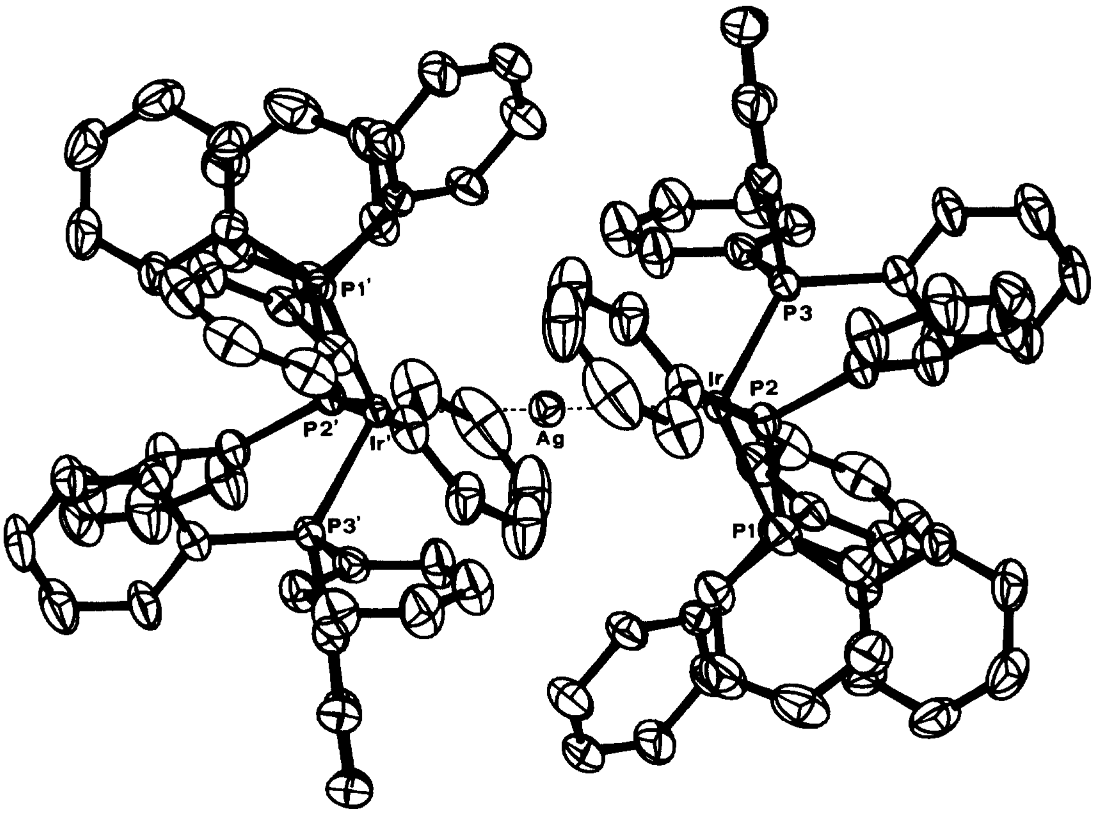

Fig. 1. Perspective view of the complex cation $[(PPh_3)_3Ir(\mu\text{-}H)_3Ag(\mu\text{-}H)_3Ir\text{-}(PPh_3)_3]^+$. The ellipsoids represent 30% probability.

of discrete ions with no short intermolecular contacts. Figure 1 shows a view of the cationic complex and a selection of bond lengths and angles are presented in Table 3. In the $P\bar{1}$ space group the Ag atom lies at the centre of symmetry and therefore only half of the molecule is symmetry-independent.

TABLE 3. Selected bond lengths (Å) and angles (°) with their eds values in parentheses

AG–IR	2.709(1)
IR–P(1)	2.369(2)
IR–P(2)	2.362(3)
IR–P(3)	2.362(4)
P(1)–C(1)	1.83(1)
P(1)–C(7)	1.85(1)
P(1)–C(13)	1.85(2)
P(2)–C(19)	1.84(1)
P(2)–C(25)	1.85(2)
P(2)–C(31)	1.85(2)
P(3)–C(37)	1.84(1)
P(3)–C(43)	1.85(1)
P(3)–C(49)	1.85(2)
P(1)–IR–AG	111.3(1)
P(2)–IR–AG	108.2(1)
P(3)–IR–AG	117.3(1)
P(2)–IR–P(1)	104.3(1)
P(3)–IR–P(1)	107.0(1)
P(3)–IR–P(2)	107.8(1)
C(1)–P(1)–IR	120.2(3)
C(7)–P(1)–IR	114.9(4)
C(13)–P(1)–IR	114.4(5)
C(7)–P(1)–C(1)	102.6(7)
C(13)–P(1)–C(1)	102.7(6)
C(13)–P(1)–C(7)	99.1(6)
C(19)–P(2)–IR	113.5(4)
C(25)–P(2)–IR	123.2(4)
C(31)–P(2)–IR	113.2(5)
C(25)–P(2)–C(19)	101.2(7)
C(31)–P(2)–C(19)	100.6(7)
C(31)–P(2)–C(25)	102.2(7)
C(37)–P(3)–IR	113.5(6)
C(43)–P(3)–IR	114.0(6)
C(49)–P(3)–IR	123.1(4)
C(43)–P(3)–C(37)	99.8(5)
C(49)–P(3)–C(37)	102.7(7)
C(49)–P(3)–C(43)	100.5(7)

The structure consists of a linear trimetallic chain in which the triphosphines adopt a staggered rotational conformation. The two pseudo C_3 axes of the $Ir(PPh_3)_3$ units are coincident with the Ir–Ir direction, so that the whole trimetallic complex possesses an approximately C_3 axis, which, with the addition of the crystallographic centre of symmetry, results in an overall C_{3i} symmetry (Fig. 2).

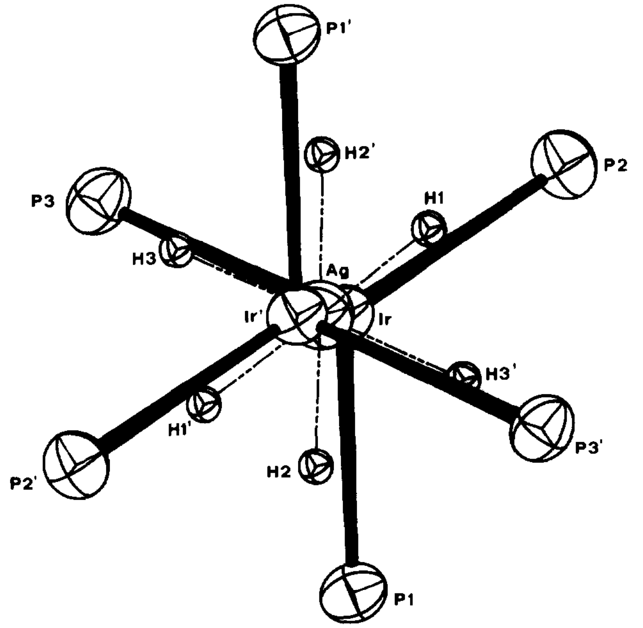

Fig. 2. View down the Ir–Ag–Ir direction of complex 1. The H atoms are at calculated positions with theoretical isotropic thermal parameters.

Although the hydride ligands were not located, the iridium atoms can be considered octahedrally coordinated in a *fac* configuration by the hydrides and by the phosphorus atoms of the triphosphines.

The coordination around the Ag atom can be assumed to be distorted octahedral. Because of the overall C_{3i} symmetry, the Ir–Ag–Ir angle is 180° and the P–Ir–Ag angles can be considered to be equivalent [108.2(1), 111.3(1), 117.3(1)°]. Therefore the six hydride ligands *trans* to the P atoms can be expected to lie equally close to the Ag atom.

In order to verify this assumption, all the hydride ligands were assumed to bridge the Ir–Ag interactions and their probable positions at potential energy minima were located and optimized by the use of the HYDEX computer program [8]. All the hydrides were accommodated in the octahedral coordination spheres of the three metals with appropriate distortions to describe a double bioctahedral confacial geometry (Fig. 3(a)). The differences in the P–Ir–Ag angles, in particular P(2)–Ir–Ag [117.3(1)°], did not sensibly affect the positions of the hydrides. The hydride ligands were then assumed to be terminally bonded to the Ir atoms and in semibridging contacts around the Ag atom. Their probable positions found by HYDEX are depicted in Fig. 3(b). In both limiting cases, all the six hydride ligands were found to fit equally well the symmetrical arrangement of the heavy atoms.

A rather different stereochemistry is present in the analogous Ir/Cu complex $[(Me_2PhP)_3HIr(\mu\text{-}H)_2Cu(\mu\text{-}H)_2IrH(Me_2PhP)_3]^+$, 2, [2]. The two phosphines assume an eclipsed rotational conformation and their pseudo-axes are bent with respect to the Ir–Cu–Ir direction, so that the six P–Ir–Cu angles are no longer equivalent: two of them are smaller and four are bigger. Because of the four bigger angles, the hydrides *trans* to the P atoms lie closer to the Cu atom and yield a distorted tetrahedral arrangement around it (the hydride positions in Fig. 4(a) were obtained by HYDEX).

In the Rh complexes **3** and **4** the P–Rh–M angles are also of two kinds, so that only four hydride ligands appear to interact with the central atom. However the P atoms of the tridentate phosphines, triphos, are almost staggered and their axes are bent towards the Rh–M–Rh axis, which in turn is not linear. The hydride ligands *trans* to the P atoms are arranged around the central atom (Ag in **3** and Cu in **4**) like the F atoms in SF_4, with two atoms at 180° and the other two on an approximately normal plane (the hydride positions in Fig. 4(b) were obtained by HYDEX).

The Ir–Ag distance is 2.709(1) Å, significantly shorter than the few other Ir–Ag distances known, and can be considered indicative of metal–metal bonding.

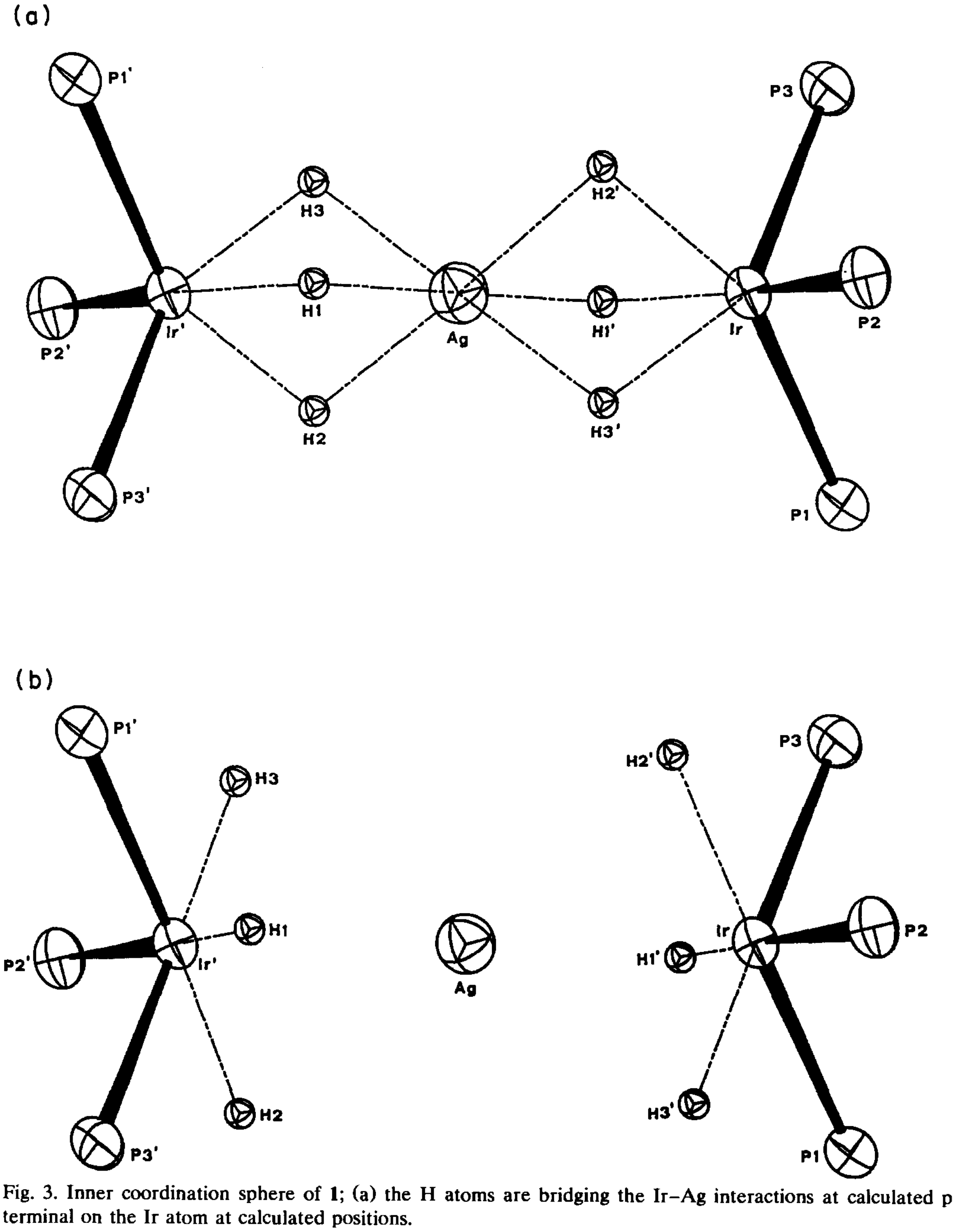

Fig. 3. Inner coordination sphere of **1**; (a) the H atoms are bridging the Ir–Ag interactions at calculated positions and (b) the H atoms are terminal on the Ir atom at calculated positions.

In $[(PPh_3)Ag(\mu\text{-}H)IrH_2(PPh_3)_3]^+$ the Ir/Ag distance is 2.758(2) Å [9] and in $[(PPh_3)_3Ir(\mu_3\text{-}H)(\mu\text{-}H)_2Ag_2(OSO_2CF_3)(H_2O)]^+$ it is equal to 2.808(4) and 2.764(4) Å [10]. In the similar Rh/Ag linear trimetal complex $[(triphos)HRh(\mu\text{-}H)_2Ag(\mu\text{-}H)_2RhH(triphos)]^+$, **3**, the Rh–Ag distance, 2.683(3) Å, is comparable with the Ir–Ag distance in **1**, whereas in the related complex **2** the Ir–Cu distances, 2.502(4) and 2.529(4) Å, are shorter. The differences between the Ir–Ag and the Ir–Cu distances are of the same order of magnitude as the differences in the ionic radii of the two coinage metals, so that both distances can be considered to reflect an interaction of comparable strength between metals.

The three Ir–P bond distances are equivalent [2.369(2), 2.362(3), 2.362(4) Å], mean 2.364 Å, and fall in the middle part of the range of values, 2.29–2.42 Å, found in triphenylphosphineiridium(III) complexes [11]. The values are equivalent within the accepted error to the value of 2.347(3) Å found for Ir–P with P *trans* to H in the monomeric complex *mer*-$[(Ph_3P)_3IrH_3]$ [12] while a shortening should be expected as a consequence of the small *trans* influence exerted by the bridging compared to the terminal hydride ligands. In the related Ir/Cu complex **2**, the Ir–P bond distances are in the expected range for the alkylarylphosphine. In particular the Ir–P bond distances with P trans to H-bridge, which average 2.297 Å, are close to the values found for dimethylphenylphosphine in other Ir complexes, although they are spread over a large range [2.277(8) to 2.316(9) Å] and are affected by large errors. In the monomeric complex *fac*-$[(Me_2PhP)_3IrH_3]$, the Ir–P bond distances average 2.294 Å [13] and in the binuclear complex $[\{IrH_3(PMe_2Ph)_2\}_2]$ the Ir–P bond distance with P *trans* to H-terminal is 2.315(2) Å [14]. In this last complex the Ir–P bond distance with P *trans* to H-bridge is significantly shorter, 2.231(3) Å, than the Ir–P bond distance with P *trans* to H-terminal, whereas in the Ir/Cu complex **2** this shortening is not detectable.

The Ir complexes with monodentate phosphines (**1** and **2**) are characterized by a linear or quasi-linear arrangement of the metals [Ir–Ag–Ir = 180° in **1** and Ir–Cu–Ir = 176° in **2**], while in the Rh complexes with the tridentate phosphine triphos (**3** and **4**) there is a greater deviation from linearity [Rh–Ag–Rh = 170.3°

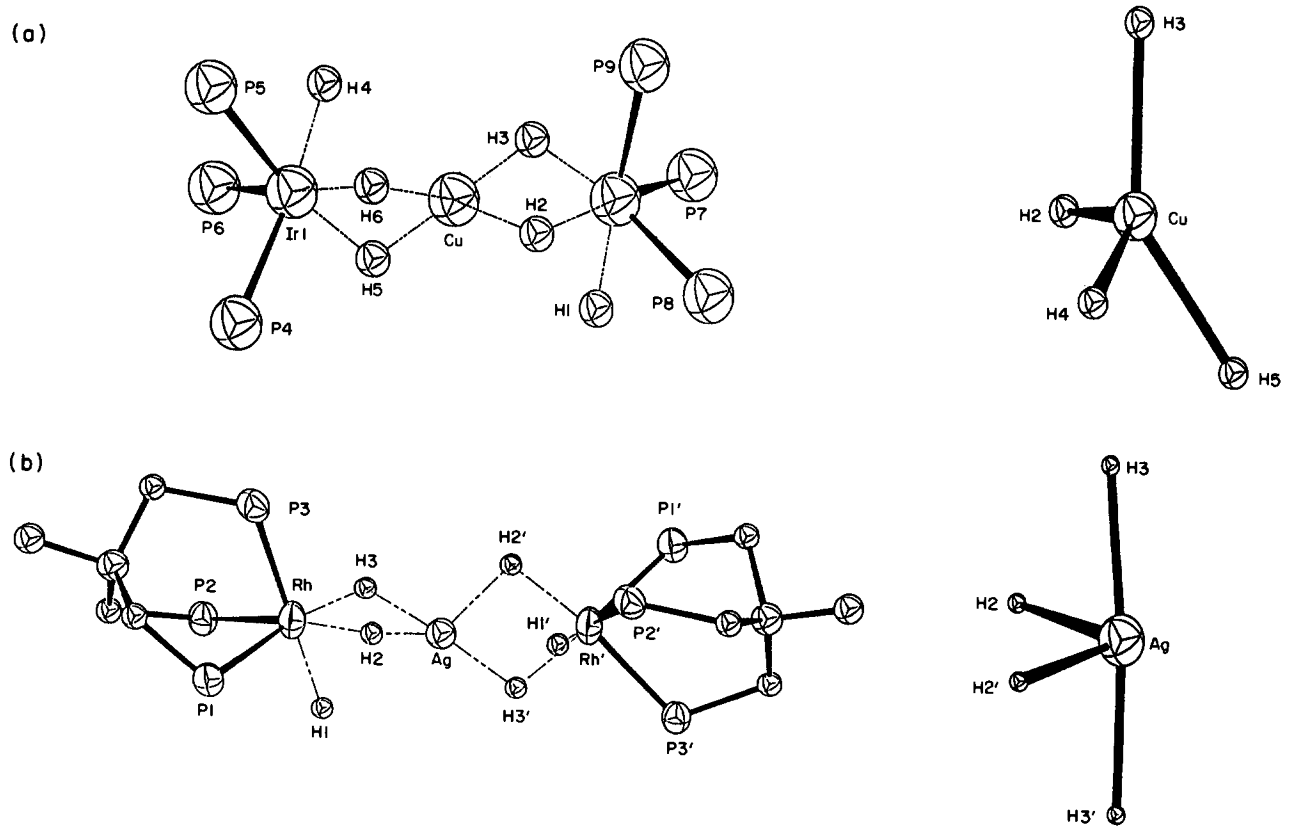

Fig. 4. (a) Inner coordination sphere of **2** with four H atoms at calculated bridging positions and two at calculated terminal positions. Also the tetrahedral coodination around the Cu atom is shown. (b) Inner coordination sphere of **3** with four H atoms at calculated bridging position and two at calculated terminal positions. The detail of the coordination around Ag is also shown.

in **3** and Rh–Cu–Rh = 168° in **4**]. In three of the complexes bridging and terminal hydride ligands are detected by IR spectroscopy and indicated by the arrangement of the heavy atoms, which suggests an SF_4-type of coordination for the central atom in **3** and **4** and a distorted tetrahedral arrangement for **2**. In **1** the presence of terminal hydride ligands suggested by IR spectroscopy is not confirmed by the structural data and the central Ag atom seems surrounded by six hydrides in an unusual octahedral arrangement.

In these four complexes the only common feature is the short Rh–M and Ir–M distances. Strong direct metal–metal interactions are postulated in addition to those present in the H-bridge interactions. A metal–metal bond can be considered the main feature of these linear clusters, while the steric differences between the phosphine and packing forces can cause the other differences observed.

Acknowledgement

The author thanks Professor L.M. Venanzi for providing samples of the compounds and for helpful discussion.

References

1 P.N. Jansen, Ph.D. Dissertation no. 8790, ETH, Zurich, 1989.
2 L.F. Rhodes, J.C. Huffman and K.J. Caulton, *J. Am. Chem. Soc., 107* (1985) 1759.
3 F. Bachechi, C. Bianchini and A. Meli, *Inorg. Chim. Acta, 213* (1993) 269.
4 F. Bachechi, L. Zambonelli and G.J. Marcotrigiano, *Cryst. Mol. Struct., 7* (1977) 11.
5 L.E. McCandlish, G.H. Stout and L.C. Andrews, *Acta Crystallogr., A24* (1968) 351.
6 A.C.T. North, C.D. Phillips and S.F. Mathews, *Acta Crystallogr., A24* (1968) 351.
7 *International Tables for X-ray Crystallography,* Vol. IV, Kynoch, Birmingham, 1974.
8 A.G. Orpen, *J. Chem. Soc., Dalton Trans.,* (1980) 2509.
9 A. Albinati, C. Anklin, P. Janser, H. Lehener, D. Matt, P.S. Pregosin and L.M. Venanzi, *Inorg. Chem., 28* (1989) 1105.
10 P. Braunstein, T.M. Gomer Carneiro, D. Matt, A. Tiripicchio and M. Tiripicchio Camellini, *Angew. Chem., Int. Ed. Engl., 25* (1986) 746.
11 G.B. Robertson and P.A. Tucker, *Acta Crystallogr., B37* (1981) 814.
12 G.R. Clark, B.W. Skelton and T.M. Waters, *Inorg. Chim. Acta, 12* (1975) 235.
13 R. Bau, W.E. Carroll, D.W. Hart and R.G. Teller, Transition metal hydrides, *Adv. Chem. Ser., 167* (1978) 73.
14 G.B. Robertson and P.A. Tucker, *Aust. J. Chem., 37* (1984) 257.